4C Code Analysis of High-Margin Quench Propagation in a DEMO TF Coil

4C Code Analysis of High-Margin Quench Propagation in a DEMO TF Coil

Roberto Zanino, Roberto Bonifetto, Laura Savoldi
Dipartimento Energia, Politecnico di Torino
Torino, Italy
roberto.zanino@polito.it

Luigi Muzzi
ENEA
Frascati, Italy

***Abstract*— In the frame of the European DEMO reactor activities, Work Package MAG, superconducting Toroidal Field (TF) coils composed by a graded (Nb3Sn + NbTi) winding pack (WP) without radial plates, encapsulated in a steel casing, are under analysis. The ENEA WP design consists of double-layer wound rectangular cable-in-conduit conductors (CICC), for which operational as well as accidental transients must be carefully investigated. The paper presents the application of the state-of-the-art thermal-hydraulic code 4C to the analysis of the quench propagation inside the WP proposed in 2014 by ENEA. The quench is conservatively initiated at the location of the maximum temperature margin and the voltage, normal zone, hot spot temperature and maximum pressure evolutions in the WP are computed, highlighting the role of thermal coupling inside the WP.**

Keywords*— *DEMO, superconducting magnets, quench, thermal-hydraulic analysis

I. Introduction

While ITER is being built in Cadarache, France, a European "roadmap to fusion electricity by 2050" has been recently proposed and approved by the European Commission [1]. It foresees the design of the DEMO reactor, see Fig. 1, as the step following ITER, aimed at the production of electricity from fusion energy.

According to the current design, the DEMO toroidal field (TF) magnets should be composed by a graded (Nb3Sn + NbTi) winding pack (WP) without radial plates, encapsulated in a steel casing [3]. The WP design proposed by ENEA in 2014 consists of double-layer wound rectangular cable-in-conduit conductors (CICC) [4], [5], to be cooled by Supercritical Helium (SHe) at 4.5 K and 0.6 MPa. Such a big difference with respect to the ITER (pancake wound) TF magnets requires a new detailed analysis of operational and accidental transients, to be performed with reliable numerical tools.

The 4C code [6], developed in the past years at Politecnico di Torino, is the state-of-the-art tool for the thermal-hydraulic analysis of SC magnet systems for fusion applications, validated against different types of transients [7], [8], [9], [10] and already applied to the investigation of the quench propagation in an ITER TF magnet [11]. The 4C code is applied here to the analysis of the quench propagation inside the DEMO TF WP proposed in 2014 by ENEA. First the 4C model of the TF conductor and WP is presented, then the setup of quench simulation is described and the results are shown.

II. 4C Model of the DEMO TF Conductor and WP

A. CICCs model

The rectangular conductor of the ENEA 2014 design, with a single central pipe as pressure relief and low-impedance path, see Fig. 2, is modeled by 4C as a standard ITER-like CICC. Transient 1D heat conduction equations describe the evolution of the temperature in the jacket and in the strands, respectively, while two sets of 1D Euler-like sets of equations account for the transient evolution of velocity, pressure and temperature in the bundle (B) and central channel (H) regions, respectively. The main geometrical parameters of the cables are given in Table 1.

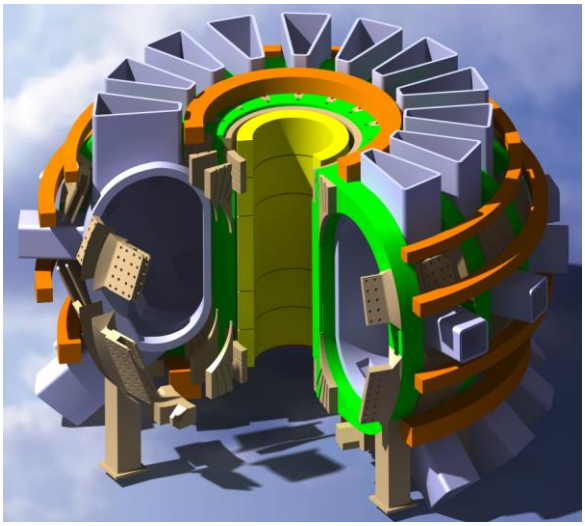

Fig. 1. The European DEMO reactor. [2]

Work partially funded by EUROfusion

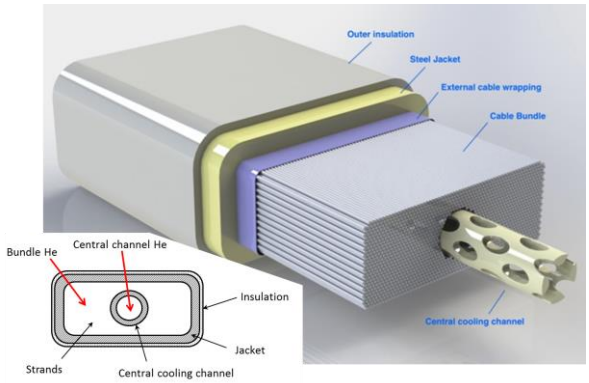

Fig. 3. ENEA CICC for the innermost layer of the European DEMO TF WP [4] (the cross section in the inset highlights the different CICC components).

Standard friction factor correlations are adopted, i.e. the Darcy-Forcheimer correlation for the flow in porous media [12] in the B [13], and the Bhatti-Shah correlation for smooth tube [14] in the H, while the convective heat transfer is computed according to the Dittus-Boelter correlation [15] in both B and H. The transfer of mass, momentum and heat between B and H is allowed through the perforated surface of the central tube, and it is driven by the local pressure difference [16]. The heat transfer through the thick wall of the central tube is also taken into account using a simple cylindrical thermal-resistance model.

The scaling describing the SC properties of the Nb3Sn is the ITER style I_c (B, T, ε) 2008 parametrization [17], with the parameters of the EUTF4-OST sample [18]: C_0 = 7.5448×10^{10} AT/m^2, B_{c20max} = 32.97 T, T_{c0max} = 16.06 K, C_{a1} = 44.48, C_{a2} = 0.0, ε_{0a} = 2.56×10^{-3}, ε_m = –4.9×10^{-4}, p = 0.63, q = 2.1. For the NbTi, the SC properties are described through the characterization reported in [19], with the following parameters: C_0 = 1.68512×10^{11}, AT/m^2, B_{c20max} = 14.61 T, T_{c0max} = 9.03 K, α = 1.0, β = 1.54, γ = 2.1, taken from values for VNIIM strands of ITER Poloidal Field coils 1 and 6 [20]-[21], as suggested in [22]. The conductor n-value is 21.5, 28.6, 31.0, 33.0, 36.9, 40.1, 12.5 and 30.1 for DL1-DL8, respectively [22]. The assumed strain value is –0.55 % for all DLs.

Table 1 – Geometrical input parameters for the DL 1.1 conductor of the DEMO TF

Hydraulic ch.	Length [m]	548.1
Central cooling channel	Inner diameter [mm]	6
	Outer diameter [mm]	10
	Tube wall perforation (pre-machined holes, see Fig. 2)	0.4
Jacket	Internal dimensions [mm]	25.8 × 69.4
	Internal curvature radius [mm]	5
	Thickness [mm]	8.7
Wrapping	Area [mm^2]	23.8
Turn insulation	External dimensions [mm]	45.2 × 88.8
	Thickness [mm]	1
Cosθ		0.95
SC strands	Number	1050
	Diameter [mm]	1
	Cu/nonCu ratio	1
Cu segregated strands	Number	462
	Diameter [mm]	1

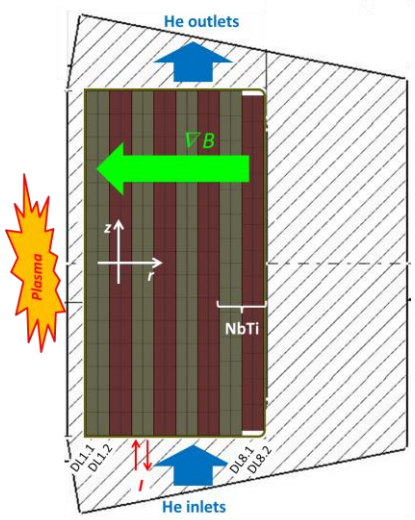

Fig. 2. Schematic view of the ENEA WP design for the European DEMO. The two conductors in the same double layer (DL) are named DLX.1 or 2.

B. *WP model*

The 16 hydraulic paths constituting the TF WP are wound in double layers DLs (each DL being a single conductor) as shown in Fig. 3, with the inlets and the outlets located at the bottom and top of the winding, respectively. The structure of the coil leads to thermal coupling between neighboring turns of the same layer and between neighboring layers. The thermal

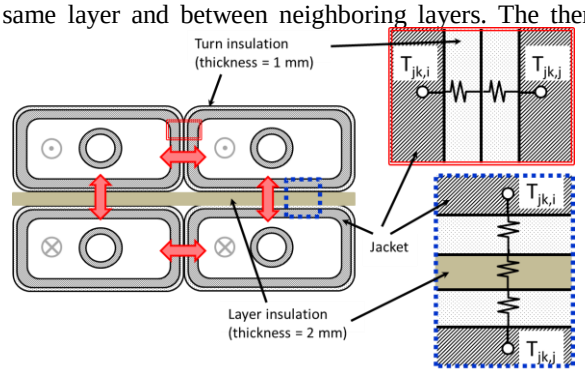

Fig. 4. Schematic view of the model for the thermal coupling between conductors in the WP.

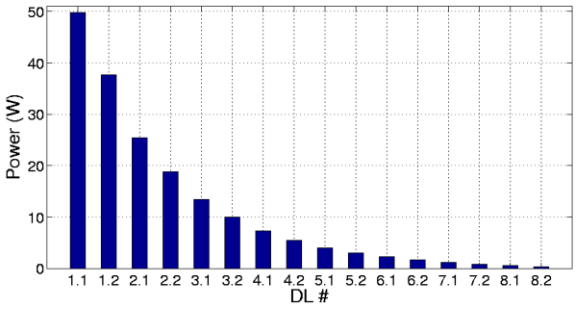

Fig. 5. Heat load foreseen for each layer.

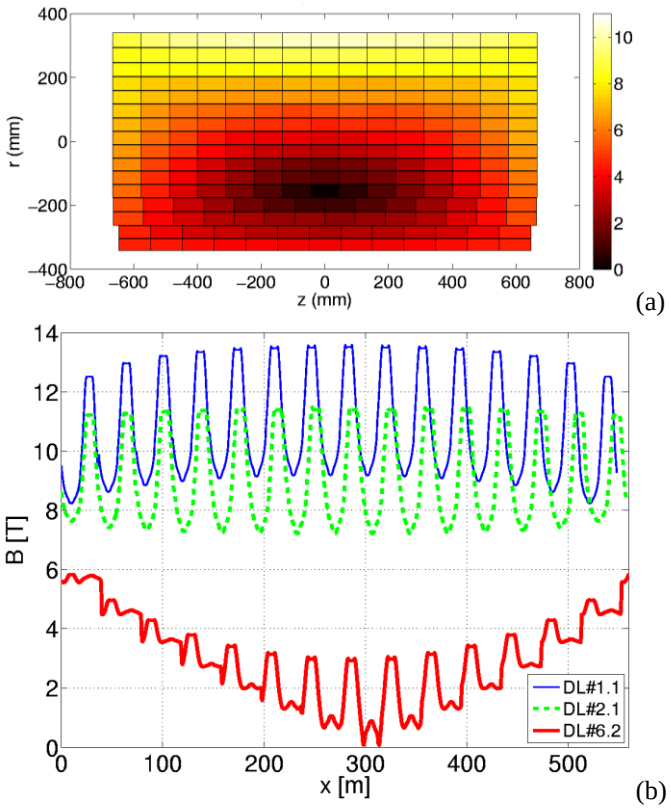

Fig. 6. Peak magnetic field in the WP: (a) map on the winding cross section at the ΔT_{mar}^{max} poloidal location; (b) distribution along the axis of selected conductors.

coupling between neighboring turns of the same layer (co-current heat transfer) and between neighboring layers (locally in counter-current) is modeled here by a series of thermal resistances [23], see Fig 4.

The inclusion of the casing as well as of the external cryogenic circuit in the model is beyond the scope of this first work on this topic and will be considered in the future. In particular, the fixed boundary conditions will cause a non-conservative overestimation of the quench propagation speed.

III. Quench Simulation Setup

The quench simulation is performed starting from the following "reference conditions":

- Initial transport current I = 81.7 kA.
- Quench detection threshold set at 0.5 V, with a delay τ_{del} = 2 s before the current dump.
- Magnetic field distribution in the WP from [24], as reported in Fig. 6.
- Inlet temperature 4.5 K, inlet pressure 0.6 MPa.
- Mass flow rate 6 g/s in each Nb3Sn layer (8 g/s in each NbTi layer).
- Uniform nuclear heat load on each layer, as estimated in [25], see Fig. 5. We neglect here the contribution to the WP heating due to the thermal coupling to the inner side of the casing, where the largest nuclear heat load would be deposited. (We assume that an independent cooling circuit for the casing should remove that load.)

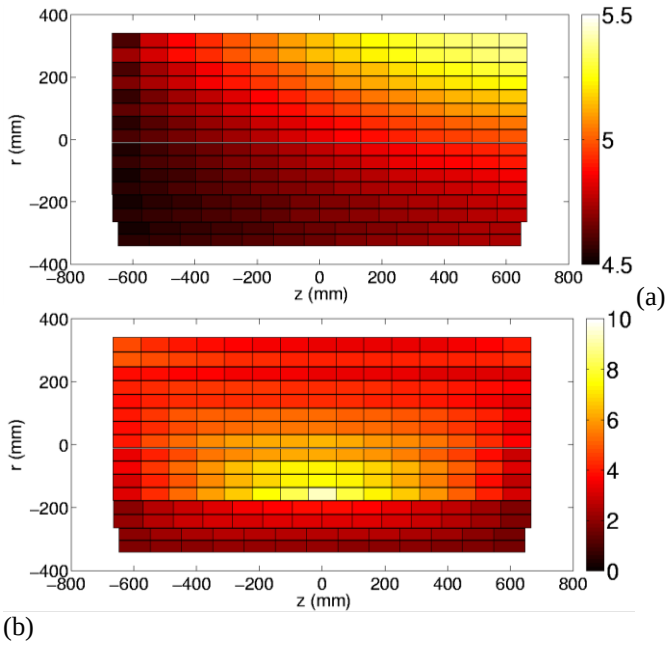

Fig. 7. Initial condition for quench propagation analysis: (a) computed temperature distribution and (b) computed ΔT_{mar} distribution in the WP at the ΔT_{mar}^{max} poloidal location.

The quench is initiated after a steady-state is reached in the WP during plasma operation, which corresponds to the initial temperature distribution used for the quench simulation in the WP shown in Fig. 7a, where the coldest zone corresponds to the inlet region while the hottest zone is computed at the outlet location of the first layers, where the nuclear load is higher (see again Fig. 5). The temperature margin ΔT_{mar} in the initial condition is shown in Fig. 7b: the minimum ΔT_{mar} (~0.7 K) is located as expected in the inner layers, while the maximum ΔT_{mar} (~9.4 K) corresponds to the outer Nb3Sn layer, in DL6.2. In order to be conservative, i.e. to capture the conditions where a quench would propagate for the longest time before detection, leading thus to the highest hot spot temperature in the WP, we simulate the quench initiation at the location of the maximum ΔT_{mar}, by means of a localized heating of 54 kW/m on a length of 1 m for 100 ms (corresponding to twice the computed Minimum Quench Energy). After 100 ms also the nuclear heating is conservatively switched off, and the quench propagates at constant current up to τ_{del}. The current is then dumped with an exponential decay, with time constant of 23 s, but the corresponding AC losses are not included in the present study.

IV. Discussion of the Computed Results

A selection of the computed results is shown in Figs. 8-10. In Fig. 8 the computed voltage evolution in the different DLs shows clearly that, although the quench is initiated in the DL6.2, the neighboring DLs are also progressively affected, see also Fig. 9. The quench is propagated there only by thermal conduction (not shown). The hot spot peak is ~260 K in DL6.2, see Fig. 10, computed during the dump (i.e., it is

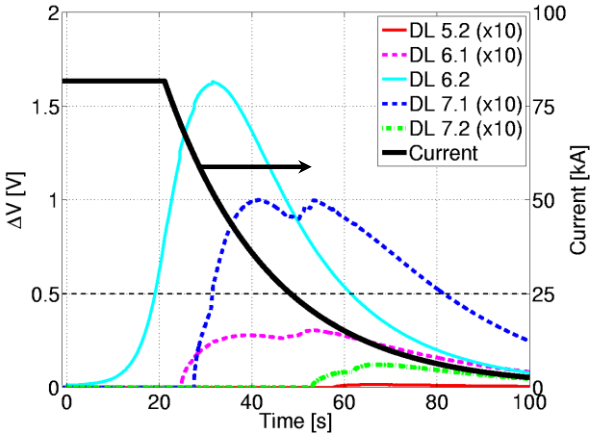

Fig. 8. Computed voltage evolution in the DLs involved by the quench (left axis) and current evolution (right axis) during the quench.

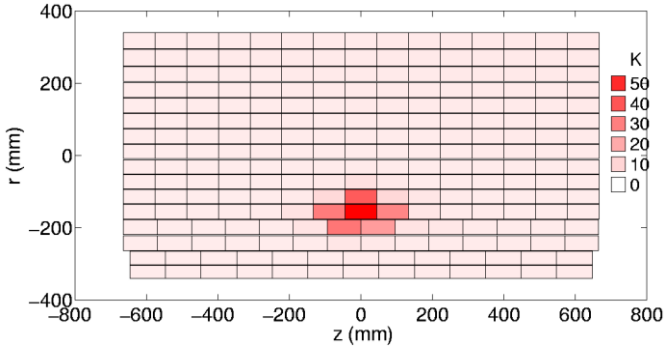

Fig. 9. Map of the computed temperature in the WP at the time of the current dump.

underestimated by neglecting the AC losses), while the peak pressurization (~2.5 MPa) occurs during the heating phase.

V. Conclusions

The first quench propagation analysis performed with the 4C code on a DEMO TF winding pack (ENEA 2014 design) has been presented.

The quench was conservatively initiated at the location of the maximum margin. With the quench detection system parameters adopted here and neglecting the AC loss generation during the dump, the simulation gives $T_{\text{hot spot}} >$ 260 K, which needs attention.

Acknowledgment

This work has been carried out within the framework of the EUROfusion Consortium and has received funding from the Euratom research and training programme 2014-2018 under grant agreement No 633053. The views and opinions expressed herein do not necessarily reflect those of the European Commission.

References

[1] F. Romanelli, et al., “Fusion electricity. A roadmap to the realisation of fusion energy”, https://www.euro-fusion.org/wpcms/wp-content/uploads/2013/01/JG12.356-web.pdf

[2] S. Turtù, A. Anemona, M. E. Biancolini, and C. Brutti, “Electromagnetic and Mechanical Analysis of candidate prototype LTS conductors, winding pack and TF coil casing”, EFDA_D_2LNP3B v2.0, 22/12/2013.

[3] EFDA PPPT, “DEMO geometry derivation from PROCESS code based on the current knowledge”, EFDA_D_2LFUG2, 30/04/2014.

[4] L. Muzzi, “Design of TF Winding Pack Option 2 (WP#2) and of “ENEA” LTS cable”, EFDA_D_2HEYFG, 23/01/2015.

[5] P. Bruzzone, K. Sedlak, D. Uglietti, N. Bykovsky, L. Muzzi, G. De Marzi, G. Celentano, A. della Corte, S. Turtù, and M. Seri, “LTS and HTS High Current Conductor Development for DEMO”, submitted to Fus. Eng. Des., 2015.

[6] L. Savoldi Richard, F. Casella, B. Fiori, and R. Zanino, “The 4C Code for the Cryogenic Circuit Conductor and Coil modeling in ITER”, Cryogenics, vol. 50, pp. 167–176, 2010.

[7] R. Zanino, R. Bonifetto, R. Heller, and L. Savoldi Richard, "Validation of the 4C Thermal-Hydraulic Code against 25 kA Safety Discharge in the ITER Toroidal Field Model Coil (TFMC)", IEEE Trans. Appl. Supercond., vol. 21, pp. 1948–1962, 2011.

[8] R. Bonifetto, A. Kholia, B. Renard, K. Riβe, L. Savoldi Richard, and R. Zanino, “Modeling of W7-X superconducting coil cool-down using the 4C code”, Fus. Eng. Des., vol. 86, pp. 1549–1552, 2011.

[9] R. Zanino, R. Bonifetto, F. Casella, and L. Savoldi Richard, “Validation of the 4C code against data from the HELIOS loop at CEA Grenoble”, Cryogenics, vol. 53, pp. 25–30, 2013.

[10] R. Zanino, R. Bonifetto, C. Hoa, and L. Savoldi Richard, “Verification of the Predictive Capabilities of the 4C Code Cryogenic Circuit Model”, AIP Conference Proceedings, vol. 1573, pp. 1586–1593, 2014.

[11] R. Zanino, D. Bessette, and L. Savoldi Richard., “Quench analysis of an ITER TF coil”, Fus. Eng. Des., vol. 85, pp.752–760, 2010.

[12] M. Bagnasco, L. Bottura, and M. Lewandowska, “Friction factor correlation for CICC’s based on a porous media analogy”, Cryogenics, vol. 50, pp. 711–719, 2010.

[13] R. Zanino, and L. Savoldi Richard, “A review of thermal-hydraulic issues in ITER cable-in-conduit conductors”, Cryogenics, vol. 46, pp. 541–555, 2006.

[14] B. R. Munson, T. H. Okiishi, W. W. Huebsch, and A. P. Rothmayer, Fluid Mechanics. Hoboken, NJ, USA: Wiley, 2013.

[15] F. P. Incropera, and D. Dewitt, Fundamentals of Heat and Mass Transfer, 6th ed., Wiley & Sons, New York, USA, 2006.

[16] R. Zanino, S. De Palo, and L. Bottura, “A two-fluid code for the thermohydraulic transient analysis of CICC superconducting magnets”, J. Fus. Energy, pp. 14–25, 1995.

[17] L. Bottura, and B. Bordini, “Jc (B, T, ε) Parameterization for the ITER Nb3Sn Production”, IEEE Trans. Appl. Supercond., vol. 19, pp. 1521–1524, 2009.

[18] A. della Corte, et al., “Successful performances of the EU-AltTF sample, a large size Nb3Sn cable-in-conduit conductor with rectangular geometry”, Supercond. Sci. Technol., vol. 23, pp. 045028, 2010.

[19] L. Bottura, “A Practical Fit for the Critical Surface of NbTi”, IEEE Trans. Appl. Supercond., vol. 10, pp. 1054–1057, 2000.

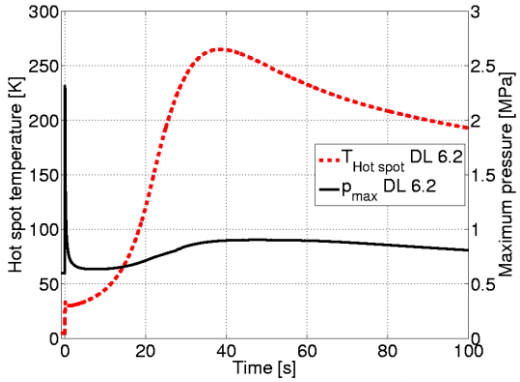

Fig. 10. Computed hot-spot temperature evolution (left axis) and maximum pressure evolution (right axis) in DL6.2 during the quench.

[20] ITER Design Description Document (DDD), "Magnets, Conductors", ITER_D_2NBKXY v1.2 (DDD 11 -7).

[21] L. Zani, et al., “Jc(T,B) Characterization of NbTi Strands Used in ITER PF-Relevant Insert and Full-Scale Sample”, IEEE Trans. Appl. Supercond., vol. 15, pp. 3506–3509, 2005.

[22] K. Sedlak, "Analysis and Assessment of Candidate Nb3Sn Conductor Design for DEMO", EFDA_D_2M87X9, v.1.0, 12/12/2012.

[23] L. Savoldi, and R. Zanino, “M&M: Multi-conductor Mithrandir code for the simulation of thermal-hydraulic transients in superconducting magnets”, Cryogenics, vol. 40, pp. 179–189, 2000.

[24] A. Torre, Personal communication, 05/12/2014, unpublished.

[25] L. Zani, Personal communication, 21/11/2014, unpublished.